

Mathematical modeling of heat transfer in counter-current multiphase flow found in gas-drilling systems with formation fluid influx

Boyun Guo^{1,2} · Jun Li³ · Jinze Song¹ · Gao Li²

Received: 7 February 2016 / Published online: 22 June 2017
© The Author(s) 2017. This article is an open access publication

Abstract The performance of gas-drilling (drilling oil and gas wells with air, nitrogen, or natural gas) is very unpredictable in many areas due to lack of proper design of drilling parameters because of limited understanding of gas–rock interaction which requires knowledge of heat transfer in the well system. Complete analysis of rock failure requires an accurate mathematical model to predict gas temperature at the bottom hole. The currently available mathematical models are unsuitable for use for the purpose because they do not consider the effects of formation fluid influx, Joule–Thomson cooling, and entrained drill cuttings. A new analytical solution for predicting gas temperature profiles inside the drill string and in the annulus was derived in this study for gas-drilling, considering all these three effects. Results of sensitivity analyses show that formation fluid influx can significantly increase the temperature profiles in both the drill string and the annulus. The Joule–Thomson cooling effect lowers the temperature in the annulus only in a short interval near the bottom hole. The drill cuttings entrained at the bottom hole can slightly increase the temperature profile in the annulus.

Keywords Gas-drilling · Temperature · Prediction · Influx · Joule–Thomson · Cuttings

✉ Boyun Guo
guo.boyun@gmail.com

¹ Petroleum Engineering Department, University of Louisiana at Lafayette, Lafayette, LA 70508, USA

² College of Petroleum Engineering, Southwest Petroleum University, Chengdu 610500, Sichuan, China

³ College of Petroleum Engineering, China University of Petroleum, Beijing 102249, China

Edited by Yan-Hua Sun

1 Introduction

Gas (air, nitrogen, or natural gas) has been widely used as the working fluid in drilling injection wells, geothermal fluid wells, and oil and gas production wells (Lyons et al. 2009). The rate of penetration is usually more than 10 times higher in gas-drilling than in liquid-drilling (drilling with water, mud, or oil). However, the performance of gas-drilling is highly inconsistent in many areas. This is generally attributed to rock failure mechanism involving thermal effects (Li et al. 2014).

It has been commonly recognized that reducing bottom hole pressure can significantly increase the rate of penetrate. This is because the low bottom hole pressure causes a high-level imbalance of stress in the rock, making the rock softer and easier to break down under the mechanical action of drill bit teeth. The effect of bottom hole pressure on rock failure seems to explain the extremely high rates in gas-drilling (Sheffield and Sitzman 1985; Li et al. 2006; Wang et al. 2008). Zhang et al. (2012) presented their results of analytical and numerical modeling which reveal that gas-cooling to the bottom hole rock is another mechanism of rock failure in gas-drilling. It indicates that a rock layer of about 1.2 cm thick is under failure conditions due to the cooling effect. Li et al.'s (2012a) experimental data demonstrate that this thermal effect drops when the gas flow rate increases. This was interpreted as the gas “penetration” effect that pushes the temperature gradient inside the rock body. The mechanism of cooling failure of rock was verified by Zhang et al.'s (2014) experimental work that shows that the cooling effect can increase the rate of penetration by 30%. Field observations also support the hypothesis of thermal failure of rock during gas-drilling. It has been found that drill cuttings collected from gas-drilling are much smaller than those

from liquid-drilling. A comparison of drill cuttings collected from gas-drilling and liquid-drilling at similar depths in the same region showed a very significant difference (Li et al. 2013b). The drill cuttings collected from gas-drilling are dust-like and are at least thousand times smaller than the drill cuttings from liquid-drilling. The explanation to this fact is still controversial. Some researchers believe it due to the re-grinding of large cuttings at the bottom hole in the gas-drilled wells (Guo and Ghalambor 2012). However, re-grinding would significantly reduce the rate of penetration, which does not seem to occur in gas-drilling. Another explanation is the theory of cuttings crushing by the drill string and other cuttings during their flowing up the borehole annulus (Li et al. 2013b). This is possible owing to pipe vibration when the drill string rotates at high speeds. Crushing can occur between drill pipe and borehole wall, in turbulent flow of fluids, uneven borehole gauge, doglegs, etc. The significance of the cuttings crushing has not been thoroughly investigated. Li et al.'s (2013a) work indicates that the energy required to crush cuttings from 6 to 1 mm is nearly equal to the energy required to transport the cuttings from the bottom hole to the surface, which is considered to be unrealistic. A reasonable explanation is that the cuttings created by the drill bit are much smaller than 6 mm. A portion of the dust-like cuttings are created at the bottom hole due to the frictional heating effect, or thermal failure of rock. This effect is similar to the weathering effect where the temperature at the surface of rock alters rapidly, causing the rapid failure of the rock surface, generating small sands. If this is the case, the cuttings size should depend on the level of frictional heat generated at the bit teeth. A high level of frictional heat should promote generation of fine cuttings. According to the theory of frictional heat generation (Kulchytsky-Zhihailo and Evtushenko 1999; Evtushenko and Pauk 2002), the heat flux is proportional to the contact pressure (stress). The contact pressure between drill bit and rock is higher at a deep depth than that at the shallow depth in gas-drilling. This is because a low weight on the bit is used to drill soft rocks at a shallow depth with a high rate of penetration and a high weight on the bit is used to drill hard rocks at deep depths to maintain a high rate of penetration. As the weight on bit increases with depth, the contact stress (weight on bit divided by bit tooth contact area) increases, and thus the frictional heat increases. It is therefore expected that the size of drill cuttings decreases with depth. Li et al. (2012b) demonstrated the trend of change of cuttings size with depth. As the well deepens, the proportion of large-size cuttings drops and that of small cuttings increases. This trend of cuttings size change may be explained by three principles: (1) rock drillability drops with depth, (2) more cuttings collision in deep holes, and (3) more thermal

failure of rock in friction-heated deep/hard formations. The fact that cuttings are much finer in gas-drilling than in liquid-drilling at the same depth tends to support the principle of thermal failure more than the other two principles. Li et al. (2014) provided a comprehensive analysis of the thermal effect in gas-drilling. They concluded that the thermal failure process is complicated by the interference between the frictional heating and Joule–Thomson cooling to the rock surface. The Joule–Thomson cooling can promote or inhibit the thermal failure of rock at the bottom hole, depending on its degree of influence on the frictional heating. Increasing weight on bit and rotary speed will promote thermal failure of rock, but may damage the drill bit due to overheating. Adding water to the gas stream to protect the drill bit will cool down the rock, reduce the thermal failure of rock, and thus lower the rate of penetration. The thermal failure should be more pronounced in drilling shale gas formations because shales have lower tensile strength than sandstones. Obviously, in order to optimize gas-drilling parameters using the thermal effect, it is essential to be able to predict the gas temperature at the bottom hole.

A number of researchers have investigated the methods for predicting fluid temperature profiles in drilling circulation systems. Among them are Zhang et al. (2011), Hasan and Kabir (2012), Eppelbaum et al. (2014), and Kutasov and Eppelbaum (2015a, b). Unfortunately, all these methods were developed for liquid-drilling, not for gas-drilling. Two methods are found applicable to gas-drilling. They are the numerical simulator developed by Wang et al. (2007) and the analytical method presented by Li et al. (2015). The former was published in a Chinese journal, and the simulator is not accessible to the authors. The latter model treats the annular fluid as a non-flowing layer of insulation and uses equivalent thermal conductivity of the flowing fluid in the annulus. Also it does not consider the effects of formation fluid influx and drill cuttings, and it does not predict the annular temperature profile. Application of the model requires input data for the equivalent thermal conductivity of the fluid mixture in the annular space. These data are difficult to obtain, if not impossible.

A new analytical solution was derived in this study for temperature prediction, considering the flowing gas, formation fluid influx, Joule–Thomson cooling, and entrained cuttings in the annular space. It corrects the result given by Li et al.'s (2015) model by 14%.

2 Mathematical model

The temperature profiles inside the drill string and in the annular space are mainly controlled by the following six factors

- Gas injection rate that brings heat to the inside of the drill string;
- Lateral heat transfer through the drill string;
- Joule–Thomson cooling effect at bit orifices;
- Heat brought to the bottom hole by drill cuttings;
- Heat brought to the bottom annulus by the formation fluid influx; and
- Lateral heat transfer through the casing and the cement sheath.

The friction pressure loss also generates heat in the system. In the practical ranges of pressure (5 to 15 MPa) and temperature (0–100 °C), the gas density varies from 1 to 100 kg/m³ and its viscosity changes from 13.3 × 10⁻⁶ to 22.1 × 10⁻⁶ m²/s (Kadoya et al. 1985). For this dilute gas, the friction pressure loss is less than 5 MPa in the typical gas-drilling systems. Therefore, the heat generation due to friction is negligible.

The thermal conductivities of the steel drill string and gas at 50 °C are 43 and 0.0127 W/(m °C), respectively. The high contrast (>1500 times) in thermal conductivity makes the fluid in the annulus the dominating material (limiting step) for the heat conduction in the lateral direction. Therefore, the resistance to heat conduction in the drill string is negligible by comparison. The thermal conductivity of gas can be used to calculate heat flow across the drill string. The thermal conductivities of the steel casing and the cement concrete at 50 °C are 43 and 1.7 W/(m °C), respectively. The high contrast (>25 times) in thermal conductivity makes the cement sheath the dominating material (limiting step) for the heat conduction in the radial direction. Therefore, the resistance to heat conduction in the casing is negligible by comparison.

When gas is injected into a drill string, the heat brought to the inside of the string is proportional to the product of fluid heat capacity C_p and mass flow rate \dot{m}_p

$$\dot{m}_p = \rho_p Q_p \tag{1}$$

where \dot{m}_p is the mass flow rate inside the drill pipe, kg/s; ρ_p is the gas density inside the drill pipe, kg/m³; and Q_p is the volumetric flow rate inside the drill pipe, m³/s. As the gas flows down the drill pipe, the rate of heat transfer through the drill pipe is proportional to the thermal conductivity of the pipe K_p . When the drilling fluid expands below the bit orifices, its temperature drops due to the Joule–Thomson cooling effect. The downstream temperature can be expressed as (Guo and Liu 2011):

$$T_{dn} = T_{up} \left(\frac{P_{dn}}{P_{up}} \right)^{\frac{k-1}{k}} \tag{2}$$

where T_{dn} and T_{up} are the absolute temperatures in the downstream and upstream of bit orifices, respectively, °C;

P_{dn} and P_{up} are the absolute pressures in the downstream and upstream of the bit orifices, respectively, psi; and k is the specific heat ratio of gas ($k = 1.3$ for gas). The temperature drop at the bit is expressed as:

$$\Delta T_J = T_{up} - T_{dn} \tag{3}$$

where ΔT_J is the temperature drop at the bit, °C.

The gas receives heat from the entrained drill cuttings and formation oil influx. Assuming all formation fluid influx occurs at the bottom hole, the fluid temperature should change at the bottom hole in the annulus by

$$\Delta T_b = -\Delta T_J + \Delta T_c + \Delta T_f \tag{4}$$

where ΔT_b is the fluid temperature change at the bottom hole (or drill bit), °C; ΔT_c and ΔT_f are the temperature changes due to the added drill cuttings and the fluid influx, respectively, °C. It can be shown that under practical drilling conditions where the rate of penetration is less than 50 m/h, the term ΔT_c is negligible. The annulus temperature at the bottom hole T_{bh} can be expressed as:

$$T_{bh} = \frac{C_p \dot{m}_p (T_p - \Delta T_J) + C_f \dot{m}_f T_{max}}{C_p \dot{m}_p + C_f \dot{m}_f} \tag{5}$$

where T_p is the temperature of fluids inside the drill pipe, °C; C_p is the heat capacity of fluids inside the drill pipe, J/(kg °C); C_f is the heat capacity of the fluid influx, J/(kg °C); \dot{m}_f is the mass flow rate of the formation fluid influx, kg/s; and T_{max} is the geotemperature at the bottom hole depth, °C. Therefore, the temperature change at the bottom hole can be expressed as:

$$\Delta T_b = T_{bh} - T_p = \frac{C_p \dot{m}_p (T_p - \Delta T_J) + C_f \dot{m}_f T_{max}}{C_p \dot{m}_p + C_f \dot{m}_f} - T_p. \tag{6}$$

The heat transfer in the annulus depends on the product of mixture heat capacity C_a and mixture mass flow rate \dot{m}_a

$$C_a \dot{m}_a = C_p \dot{m}_p + C_s \dot{m}_s + C_f \dot{m}_f, \tag{7}$$

and the product of heat capacity and mass flow rate of solid cuttings $C_s \dot{m}_s$ is further expressed in two terms:

$$C_s \dot{m}_s = C_h \dot{m}_h + C_r \dot{m}_r \tag{8}$$

where C_a is the heat capacity of fluids in the annulus, J/(kg °C); C_h is the heat capacity of hydrocarbons in the cuttings, J/(kg °C); and C_r is the heat capacity of dry rock, J/(kg °C); C_s is the heat capacity of solids in the annulus, J/(kg °C); \dot{m}_a is the mass flow rate in the annulus, kg/s; \dot{m}_h is the mass flow rate of hydrocarbons in cuttings, kg/s; \dot{m}_r is the mass flow rate of rock, kg/s; \dot{m}_s is the mass flow rate of solid cuttings in the annulus, kg/s. The mass flow rates of the hydrocarbons and rock in the cuttings are, respectively, expressed as:

$$\dot{m}_h = \frac{\pi}{4} D_b^2 R_p \varphi \rho_h \quad (9)$$

and

$$\dot{m}_r = \frac{\pi}{4} D_b^2 R_p (1 - \varphi) \rho_r \quad (10)$$

where D_b is the drill bit diameter, m; R_p is the rate of penetration, m/s; φ is the rock porosity; ρ_h is the density of hydrocarbons in cuttings, kg/m³; and ρ_r is the rock density; kg/m³. C_f in Eq. (4) is the heat capacity of formation influx fluids (usually oil), and the mass flow rate of formation fluid influx is expressed as

$$\dot{m}_f = \rho_f Q_f \quad (11)$$

where ρ_f is the density of the formation fluids, kg/m³; Q_f is the flow rate of the formation fluid influx, m³/s. As the fluid mixture flows up the annulus, the rates of heat transfer through the drill string and the cement sheath are proportional to the thermal conductivities of the drill string K_p and the cement sheath K_c , respectively (the thermal conductivity of the casing is assumed to be infinity compared to that of the cement sheath).

The gas temperatures inside the drill pipe T_p and in the annulus T_a take the following forms, respectively (derivation of the solution is given in Appendix):

$$T_p = C_1 A e^{r_1 L} + C_2 A e^{r_2 L} + GL + \frac{AG + AB T_{g0} - G(B + E)}{AB} \quad (12)$$

and

$$T_a = C_1 (A + r_1) e^{r_1 L} + C_2 (A + r_2) e^{r_2 L} + GL + \frac{AG + AB T_{g0} - EG}{AB} \quad (13)$$

with

$$C_1 = \frac{AB(A\Delta T_b - G) - [AB T_{p0} - AB T_{g0} - AG + G(B + E)] r_2 e^{r_2 L_{\max}}}{A^2 B (r_1 e^{r_1 L_{\max}} - r_2 e^{r_2 L_{\max}})} \quad (14)$$

$$C_2 = \frac{-AB(A\Delta T_b - G) + [AB T_{p0} - AB T_{g0} - AG + G(B + E)] r_1 e^{r_1 L_{\max}}}{A^2 B (r_1 e^{r_1 L_{\max}} - r_2 e^{r_2 L_{\max}})} \quad (15)$$

$$r_1 = \frac{B + E - A + \sqrt{(B + E - A)^2 + 4AB}}{2} \quad (16)$$

$$r_2 = \frac{B + E - A - \sqrt{(B + E - A)^2 + 4AB}}{2} \quad (17)$$

$$A = \frac{\pi d_p K_p}{C_p \dot{m}_p t_p} \quad (18)$$

$$B = \frac{\pi d_c K_c}{C_a \dot{m}_a t_c} \quad (19)$$

$$E = \frac{\pi d_p K_p}{C_a \dot{m}_a t_p} \quad (20)$$

where d_c is the inner diameter of the cement sheath, m; d_p is the inner diameter of the drill pipe, m; G is the geothermal gradient, °C/m; K_c and K_p are the thermal conductivities of the cement and the drill pipe, respectively, W/(m °C); L is the wellbore depth along the drill string, m; L_{\max} is the maximum hole depth, m; t_c is the thickness of the cement sheath, m; t_p is the wall thickness of the drill pipe, m; T_a is the temperature of fluids in the annulus, °C; T_{g0} is the geothermal temperature at surface, °C; T_{p0} is the temperature of fluids inside the drill pipe at surface, °C.

Because Eq. (6) involves the in-string temperature T_p at the bottom depth, it is necessary to solve Eqs. (6) and (12) simultaneously with a numerical method such as a Newton–Raphson iteration. These equations were solved in a spreadsheet program using the Goal Seek tool in MS Excel.

3 Model comparison

The newly derived analytical solution was coded in an MS Excel spreadsheet to compare with other models. A number of numerical models have been presented for fluid temperature prediction, including Keller et al. (1973), Wooley (1980), Marshall and Bentsen (1982), Kabir et al. (1996), and Hasan and Kabir (2012). Unfortunately, all these models were developed for liquid or multi-phase flow. They are not applicable to gas flow in gas-drilling. The analytical model for gas-drilling presented by Li et al. (2015) was used for comparison. The data used in the models are provided in Table 1.

Nitrogen is the major component of air (>78%). Heat capacity of N₂ is a function of temperature and pressure (Abbott and van Ness 1989). In the temperature range between 0 and 100 °C at atmospheric pressure, the heat capacity of air varies between 1005 and 1009 J/(kg °C), or within 0.40%. In gas-drilling operations, the gas pressure in the drill string is in a narrow range between 7 and 10 MPa. The heat capacity of the gas varies between 1016.2 and 1021.6 J/(kg °C), or within 0.53%, in this pressure range (Kadoya et al. 1985). Considering the extreme condition of 0 °C and 10 MPa, the heat capacity of gas varies between 1005 and 1021.6 J/(kg °C), or within 1.65%. Therefore, the heat capacity of gas was assumed to be constant in this study.

Figure 1 indicates that the injected gas is cooled down in the upper section of the drill string by the geothermal gradient. Gas is then heated up by the geothermal gradient in the lower section of the drill string. After arrival in the annulus, the gas is quickly heated up by the geothermal

Table 1 Data used in comparison of analytical solutions

Factor	Value
Depth L , m	2000
Bit diameter D_b , m	0.201
Inner diameter of the cement d_c , m	0.245
Outer diameter of the cement D_c , m	0.311
Outer diameter of the drill string D_p , m	0.114
Inner diameter of the drill string d_p , m	0.098
Geothermal temperature at surface T_{g0} , °C	20
Geothermal gradient G , °C/m	0.0245
Thermal conductivity of the cement K_c , W/(m °C)	1.2
Thermal conductivity of the drill pipe K_p , W/(m °C)	42
Injection rate Q_p , m ³ /s	2.26
Temperature of the injected fluid T_{p0} , °C	40
Heat capacity of the fluid inside the pipe C_p , J/(kg °C)	1005
Heat capacity of rock C_r , J/(kg °C)	920
Heat capacity of the formation fluid C_f , J/(kg °C)	1880
Porosity φ	0.3
Rate of penetration R_p , m/h	10
Temperature drop at the bit T_b , °C	0
Density of rock ρ_r , kg/m ³	2650
Density of the formation fluid ρ_f , kg/m ³	1000
Density of the injected fluid ρ_p , kg/m ³	1.127
Formation fluid influx rate Q_f , m ³ /s	0.005

gradient in the lower section of the annulus. Eventually, the gas is cooled down in the upper section of the annulus by the geothermal gradient.

Also presented in Fig. 1 is the gas temperature profile inside the drill string given by Li et al.’s analytical model (Li et al. 2015). It is seen that the bottom hole temperature given by the new analytical model is much closer to the geothermal temperature than that given by Li et al.’s model. It can be explained that the main heat source

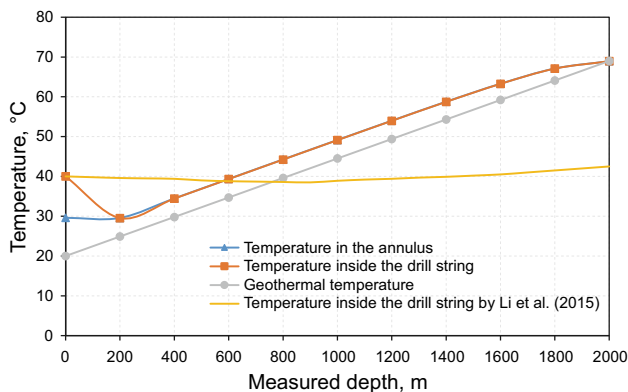


Fig. 1 A comparison of temperature profiles given by different analytical models

coming into the drilling system is the heat from the formation (heat transfer and formation fluid/cuttings). The temperature profiles both in the annulus and inside the drill string should be close to the geothermal temperature, especially for the temperature in the annulus because the heat can pass from the formation directly and drill cuttings can also bring heat directly to the annulus. Compared to the results from the Li et al. (2015) model, the new model is more reasonable. In addition, the new analytical model has the ability to simulate the temperature profile in the annulus. Li et al.’s (2015) model only can simulate the flowing fluid temperature inside the drill string. The new model, seen from the derivation, considered the heat transfer between the drill string and the annulus.

4 Sensitivity analysis

Previous models do not consider the effects of the formation fluid influx, Joule–Thomson cooling, and entrained drill cuttings at the bottom hole on the temperature profiles inside the drill string and in the annulus. These effects were analyzed with the new model in this study. Figures 2 and 3 demonstrate the effect of the formation fluid influx on the temperature profiles both in the annulus and inside the drill string. It shows that the formation fluid influx can significantly increase the temperature profiles in both the drill string and the annulus. This effect can be explained by the fact that higher formation fluid influx means more heat flow into the drilling system in the same time period. Thus, the high flow rate of formation fluid influx can make the temperature profiles closer to the geothermal temperature.

Figure 4 illustrates the effect of Joule–Thomson cooling on the temperature profiles. It is seen that the Joule–Thomson cooling effect lowers the temperature in the annulus only in the vicinity of the bottom hole. It diminishes quickly within a very short interval when the drilling

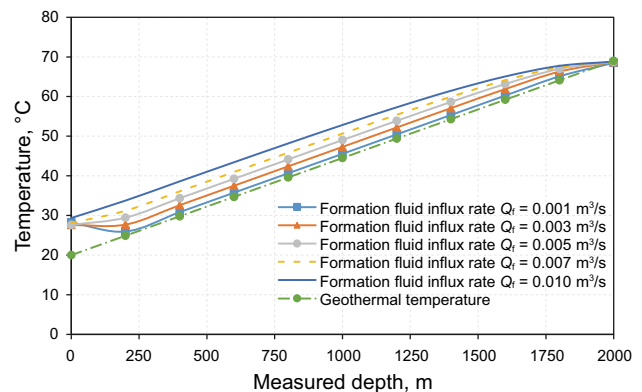


Fig. 2 Effect of the formation fluid influx on the temperature profile in the annulus

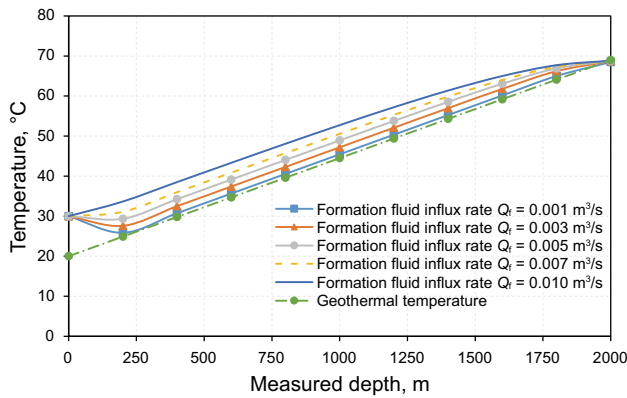


Fig. 3 Effect of the formation fluid influx on the temperature profile inside the drill string

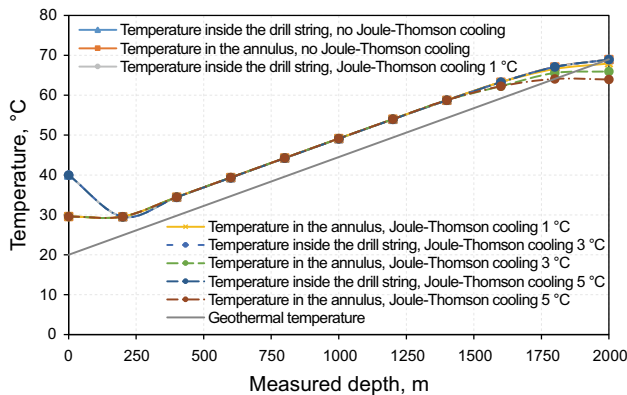


Fig. 4 Effects of Joule–Thomson cooling on the temperature profiles

fluid moves up the annulus. In other words, the Joule–Thomson cooling does not significantly affect the temperature profiles along the whole well depth except at the bottom hole. This cooling effect can be used to cool down the drill bit in drilling hard formation rocks where the overheating due to friction can cause damage to the drill bit.

Figure 5 shows the effect of entrained drill cuttings on the temperature profiles. It indicates that the drill cuttings can slightly increase the temperature profile in the annulus even at a very high rate of penetration up to 30 m/h. The comparisons among Figs. 1, 2, and 5 also demonstrate that the formation fluid influx rate (Q_f) has a much stronger effect on the temperature profiles during gas-drilling than that of the rate of penetration. The reason for this difference is analyzed as follows. The formation fluid influx rate (Q_f) can be used to show the volume of fluids coming into the drilling annulus during drilling. The rate of penetration, neglecting the friction heat, has a direct effect on

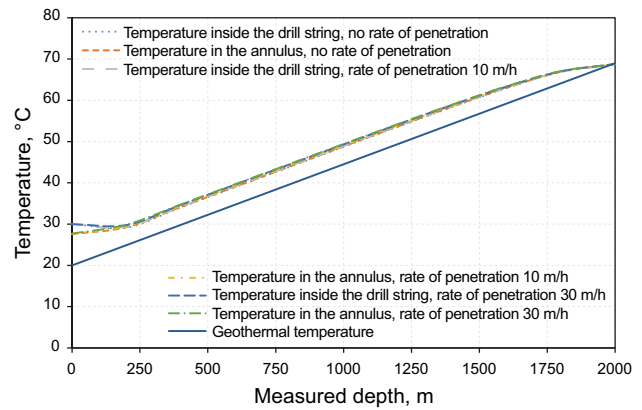


Fig. 5 Effects of entrained drill cuttings on the temperature profiles

temperature profiles by considering the volume of rock (drill cuttings) coming into the annulus at the same unit time. The mathematic relationship can be derived as follows:

$$Q_{\text{rock from formation}} = \frac{R_p}{3600} A_a = \frac{R_p}{3600} \frac{\pi(d_c^2 - D_p^2)}{4} \quad (21)$$

where A_a is the cross-sectional area of the annulus, m^2 ; D_p is the outer diameter of the drill pipe, m ; and $Q_{\text{rock from formation}}$ is the flow rate of formation rock, m^3/s .

Taking the rate of penetration as 10 m/h, the volume of rock coming into the annulus is $0.0001 m^3/s$. This number is much lower than a typical value of influx rate $Q_f = 0.005 m^3/s$. Considering the fact that the heat capacity of rock ($920 J/(kg \text{ } ^\circ C)$) is about 50% of that of the formation fluid ($1880 J/(kg \text{ } ^\circ C)$), the fluid from the formation brings much more heat into the annulus than drill cuttings.

5 Conclusions

A new closed-form analytical solution for predicting gas temperature profiles inside the drill string and in the annulus was derived in this study for gas-drilling. The new solution has advantages over the existing solution in that it can handle formation fluid influx, the Joule–Thomson cooling effect, and entrained drill cuttings. The following conclusions are drawn from this study:

- (1) An example calculation shows that the injected hot gas is cooled down in the upper section of the drill string by the geothermal gradient. Gas is then heated up by the geothermal gradient in the lower section of the drill string. After arrival in the annulus, the gas is quickly heated up by the geothermal gradient in the

lower section of the annulus. Eventually, the gas is cooled down in the upper section of the annulus by the geothermal gradient.

- (2) The temperature profiles given by the new analytical solution are significantly different from those given by Li et al.'s analytical model. If the new model is considered to be accurate, Li et al.'s (2015) model is expected to significantly underestimate the bottom hole temperature.
- (3) Results of sensitivity analyses show that the formation fluid influx can significantly increase the temperature profiles in both the drill string and the annulus. The Joule–Thomson cooling effect lowers the temperature in the annulus only in the vicinity of the bottom hole. The drill cuttings entrained at the bottom hole can slightly increase the temperature profile in the annulus.
- (4) The new analytical solution has some limitations including steady gas flow. Also it may give erroneous results if the equivalent thermal conductivity of the annular fluid is not correctly estimated. Thermal conductivity values should be adjusted based on temperature measurements in critical applications.

Direct measurement of temperature profiles is required to further validate the new analytical solution. Once validated, the new solution can replace numerical simulators that are not readily available to field engineers in general.

Acknowledgements This research was supported by the China National Natural Science Foundation Funding No. 51134004.

Open Access This article is distributed under the terms of the Creative Commons Attribution 4.0 International License (<http://creativecommons.org/licenses/by/4.0/>), which permits unrestricted use, distribution, and reproduction in any medium, provided you give appropriate credit to the original author(s) and the source, provide a link to the Creative Commons license, and indicate if changes were made.

Appendix: mathematical modeling of heat transfer in gas-drilling

Assumptions

The following assumptions are made in the model formulation:

- (a) The thermal conductivities of casings are assumed to be infinitive.
- (b) The geothermal gradient behind the annulus is not affected by the borehole fluid.
- (c) The heat capacity of fluid is constant.
- (d) Friction-induced heat is negligible.

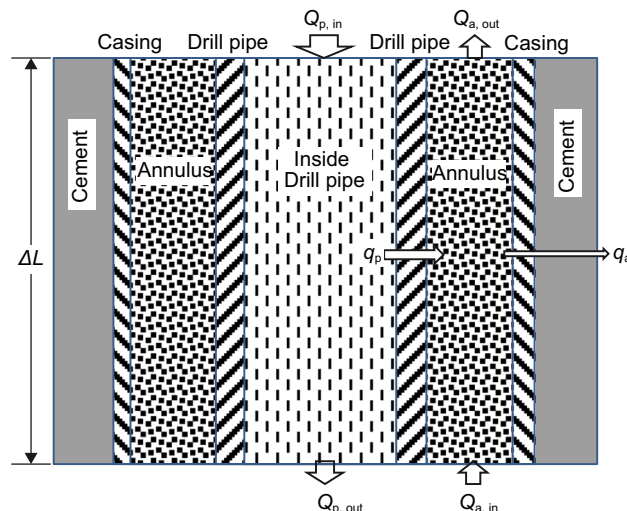


Fig. 6 Sketch illustrating heat transfer in a borehole section

Governing equation

Figure 6 depicts a small element of a borehole section with a drill string at the center.

Consider the heat flow inside the drill pipe during a time period of Δt . The heat balance is given by

$$Q_{p,in} - Q_{p,out} - q_p = Q_{p,chg} \tag{A.1}$$

where $Q_{p,in}$ is the heat energy brought into the drill pipe element by fluids due to convection, J; $Q_{p,out}$ is the heat energy carried away from the drill pipe element by fluids due to convection, J; q_p is the heat transfer through the drill pipe due to conduction, J; $Q_{p,chg}$ is the change of heat energy in the fluids in the drill pipe, J.

These terms can be further formulated as

$$Q_{p,in} = C_p \dot{m}_p T_{p,L} \Delta t \tag{A.2}$$

$$Q_{p,out} = C_p \dot{m}_p T_{p,L+\Delta L} \Delta t \tag{A.3}$$

$$q_p = \pi d_p K_p \Delta L \left(-\frac{\partial T_p}{\partial r} \right) \Delta t \tag{A.4}$$

$$Q_{p,chg} = C_p \rho_p A_p \Delta L \Delta T_p \tag{A.5}$$

where A_p is the cross-sectional area of the drill pipe, m^2 .

Substituting Eq. (A.2) through Eq. (A.5) into Eq. (A.1) gives

$$C_p \dot{m}_p \Delta t (T_{p,L} - T_{p,L+\Delta L}) + \pi d_p K_p \Delta L \left(\frac{\partial T_p}{\partial r} \right) \Delta t = \rho_p C_p A_p \Delta L \Delta T_p \tag{A.6}$$

Dividing all the terms of this equation by $\Delta L \Delta t$ yields

$$C_p \dot{m}_p \frac{(T_{p,L} - T_{p,L+\Delta L})}{\Delta L} + \pi d_p K_p \frac{\partial T_p}{\partial r} = \rho_p C_p A_p \frac{\Delta T_p}{\Delta t} \tag{A.7}$$

For infinitesimal of ΔL and Δt , this equation becomes

$$\frac{\partial T_p}{\partial L} + \frac{\rho_p A_p}{\dot{m}_p} \frac{\partial T_p}{\partial t} = \frac{\pi d_p K_p}{C_p \dot{m}_p} \frac{\partial T_p}{\partial r} \quad (\text{A.8})$$

The radial-temperature gradient in the insulation layer can be formulated as

$$\frac{\partial T_p}{\partial r} = \frac{T_a - T_p}{t_p} \quad (\text{A.9})$$

Substituting Eq. (A.9) into Eq. (A.8) yields

$$\frac{\partial T_p}{\partial L} + \lambda_p \frac{\partial T_p}{\partial t} + \alpha_p (T_p - T_a) = 0 \quad (\text{A.10})$$

where

$$\lambda_p = \frac{\rho_p A_p}{\dot{m}_p} \quad (\text{A.12})$$

$$\alpha_p = \frac{\pi d_p K_p}{C_p \dot{m}_p t_p}. \quad (\text{A.13})$$

Consider the heat flow in the annulus during a time period of Δt . Heat balance is given by

$$Q_{a,\text{in}} - Q_{a,\text{out}} + q_p - q_a = Q_{a,\text{chng}} \quad (\text{A.14})$$

where $Q_{a,\text{in}}$ is the heat energy brought into the annulus element by fluids due to convection, J; $Q_{a,\text{out}}$ is the heat energy carried away the annulus element by fluids due to convection, J; q_a is the heat transfer through casing and cement due to conduction, J; $Q_{p,\text{chng}}$ is the change of heat energy in the fluids, J.

These terms can be further formulated as

$$Q_{a,\text{in}} = C_a \dot{m}_a T_{a,L+\Delta L} \Delta t \quad (\text{A.15})$$

$$Q_{a,\text{out}} = C_a \dot{m}_a T_{a,L} \Delta t \quad (\text{A.16})$$

$$q_a = \pi d_c K_c \Delta L \left(-\frac{\partial T_a}{\partial r} \right) \Delta t \quad (\text{A.17})$$

$$Q_{a,\text{chng}} = C_a \rho_a A_a \Delta L \Delta T_a. \quad (\text{A.18})$$

Substituting Eq. (A.15) through Eq. (A.18) into Eq. (A.14) gives

$$\begin{aligned} C_a \dot{m}_a \Delta t (T_{a,L+\Delta L} - T_{a,L}) - \pi d_p K_p \Delta L \left(\frac{\partial T_p}{\partial r} \right) \Delta t \\ + \pi d_c K_c \Delta L \left(\frac{\partial T_a}{\partial r} \right) \Delta t \\ = \rho_a C_a A_a \Delta L \Delta T_a. \end{aligned} \quad (\text{A.19})$$

Dividing all the terms of this equation by $\Delta L \Delta t$ yields

$$\begin{aligned} C_a \dot{m}_a \frac{(T_{a,L+\Delta L} - T_{a,L})}{\Delta L} - \pi d_p K_p \left(\frac{\partial T_p}{\partial r} \right) + \pi d_c K_c \left(\frac{\partial T_a}{\partial r} \right) \\ = \rho_a C_a A_a \frac{\Delta T_a}{\Delta t}. \end{aligned} \quad (\text{A.20})$$

For infinitesimal of ΔL and Δt , this equation becomes

$$\begin{aligned} C_a \dot{m}_a \frac{\partial T_a}{\partial L} - \rho_a C_a A_a \frac{\partial T_a}{\partial t} - \pi d_p K_p \left(\frac{\partial T_p}{\partial r} \right) + \pi d_c K_c \left(\frac{\partial T_a}{\partial r} \right) \\ = 0. \end{aligned} \quad (\text{A.21})$$

The radial-temperature gradient in the insulation layer can be formulated as

$$\frac{\partial T_a}{\partial r} = \frac{T_g - T_a}{t_c}. \quad (\text{A.22})$$

Substituting Eqs. (A.9) and (A.22) into Eq. (A.21) yields

$$\frac{\partial T_a}{\partial L} - \lambda_a \frac{\partial T_a}{\partial t} + \beta_a (T_p - T_a) - \alpha_a (T_a - T_g) = 0 \quad (\text{A.23})$$

where

$$\lambda_a = \frac{\rho_a A_a}{\dot{m}_a} \quad (\text{A.24})$$

$$\beta_a = \frac{\pi d_p K_p}{C_a \dot{m}_a t_p} \quad (\text{A.25})$$

$$\alpha_a = \frac{\pi d_c K_c}{C_a \dot{m}_a t_c}. \quad (\text{A.26})$$

The temperatures T_p and T_a at any given depth can be solved numerically from Eqs. (A.10) and (A.23).

For steady heat flow, Eqs. (A.10) and (A.23) can be written as:

$$\frac{\partial T_p}{\partial L} + \alpha_p (T_p - T_a) = 0 \quad (\text{A.27})$$

$$\frac{\partial T_a}{\partial L} + \beta_a (T_p - T_a) - \alpha_a (T_a - T_g) = 0 \quad (\text{A.28})$$

where the geotemperature can be expressed as:

$$T_g = T_{g0} + GL. \quad (\text{A.29})$$

Boundary conditions

The boundary conditions for solving Eqs. (A.27) and (A.28) are expressed as

$$T_p = T_{p0} \quad \text{at } L = 0 \quad (\text{A.30})$$

$$T_a = T_p + \Delta T_b \quad \text{at } L = L_{\text{max}}. \quad (\text{A.31})$$

Solution

Governing equations (A.27) and (A.28) subjected to the boundary conditions [Eqs. (A.30) and (A.31)] were solved with the method of characteristics. The solutions take the following form:

$$T_p = C_1 A e^{r_1 L} + C_2 A e^{r_2 L} + aL + \frac{Aa + ABb - a(B + E)}{AB} \quad (\text{A.32})$$

$$T_a = C_1(A + r_1)e^{r_1L} + C_2(A + r_2)e^{r_2L} + aL + \frac{Aa + ABb - aE}{AB} \tag{A.33}$$

where

$$C_1 = \frac{AB(AD - a) - [ABC - ABb - Aa + a(B + E)]r_2e^{r_2L_{max}}}{A^2B(r_1e^{r_1L_{max}} - r_2e^{r_2L_{max}})} \tag{A.34}$$

$$C_2 = \frac{-AB(AD - a) + [ABC - ABb - Aa + a(B + E)]r_1e^{r_1L_{max}}}{A^2B(r_1e^{r_1L_{max}} - r_2e^{r_2L_{max}})} \tag{A.35}$$

$$r_1 = \frac{B + E - A + \sqrt{(B + E - A)^2 + 4AB}}{2} \tag{A.36}$$

$$r_2 = \frac{B + E - A - \sqrt{(B + E - A)^2 + 4AB}}{2} \tag{A.37}$$

where $A = \alpha_p$, $B = \alpha_a$, $C = T_{p0}$, $D = \Delta T_b$, $E = \beta_a$, $a = G$, and $b = T_{g0}$.

References

Abbott MM, Van Ness HC. Thermodynamics (2nd edition). New York: McGraw-Hill Publishing Company; 1989. p. 100–1.

Eppelbaum LV, Kutasov IM, Pilchin AN. Applied geothermics. Berlin: Springer; 2014. p. 751.

Evtushenko OO, Pauk VI. Steady-state frictional heat generation on a periodic sliding contact. *J Math Sci*. 2002;109(1):1266–72. doi:10.1023/A:1013757030298.

Guo B, Ghalambor A. Natural gas engineering handbook. 2nd ed. Houston: Gulf Publishing Company 2012.

Guo B, Liu G. Applied drilling circulation systems. Oxford: Elsevier; 2011. p. 145–50.

Hasan AR, Kabir CS. Wellbore heat-transfer modeling and applications. *J Pet Sci Eng*. 2012;86–87:127–36. doi:10.1016/j.petrol.2012.03.021.

Kabir CS, Hasan AR, Kouba GE, Ameen NM. Determining circulating fluid temperature in drilling, workover, and well-control operations. *SPE Drill Complet*. 1996. doi:10.2118/24581-PA.

Kadoya K, Matsunaga N, Nagashima A. Viscosity and thermal conductivity of dry air in the gaseous phase. *J Phys Chem Ref Data*. 1985;14(4):947–70. doi:10.1063/1.555744.

Keller HH, Couch EJ, Berry PM. Temperature distribution in circulating mud columns. *SPE J*. 1973;13(1):23–30. doi:10.2118/3605-PA.

Kulchitsky-Zhihailo RD, Evtushenko AA. Steady-state frictional heat generation on axisymmetric sliding contact of a thermosensitive sphere and a fixed, thermally insulated base. *J Appl Mech Tech Phys*. 1999. doi:10.1007/BF02467985.

Kutasov IM, Eppelbaum LV. Pressure and temperature well testing. Boca Raton: CRC Press (Taylor and Francis) Inc; 2015a. p. 325.

Kutasov IM, Eppelbaum LV. Wellbore and formation temperatures during drilling, cementing of casing and shut-in. In: Proceedings of the world geothermal congress, 19–25 April, Melbourne, Australia. 2015b.

Li Y, Meng Y, She Z, Zhang J. Investigations of increased rate of penetration in air drilling. *China Pet Drill Explor Technol*. 2006;34(4):9–11 (in Chinese).

Li J, Guo B, Ai C. Analytical and experimental investigations of the effect of temperature gradient on rock failure. In: ASME 2012 international mechanical engineering congress and exposition, November 9–15, Houston, Texas, 2012a. doi:10.1115/IMECE2012-86436.

Li J, Yang S, Guo B, Feng Y, Liu G. Distribution of the sizes of rock cuttings in gas drilling at various depths. *Comput Model Eng Sci (CMES)*. 2012b;89(2):79–96. doi:10.3970/cmesci.2012.089.079.

Li J, Guo B, Liu G, Liu W. The optimal range of the nitrogen-injection rate in shale-gas well drilling. *SPE Drill Complet*. 2013a;28(1):60–4. doi:10.2118/163103-PA.

Li J, Yang S, Liu G. Cutting breakage and transportation mechanism of air drilling. *Int J Oil Gas Coal Technol*. 2013b;6(3):259–70. doi:10.1504/IJOGCT.2013.052237.

Li J, Guo B, Yang S, Liu G. The complexity of thermal effect on rock failure in gas-drilling shale gas wells. *J Nat Gas Sci and Eng*. 2014;21:255–9. doi:10.1016/j.jngse.2014.08.011.

Li J, Guo B, Li B. A closed form mathematical model for predicting gas temperature in gas-drilling unconventional tight reservoirs. *J Nat Gas Sci Eng*. 2015;27:284–9. doi:10.1016/j.jngse.2015.08.064.

Lyons WC, Guo B, Graham RL, Hawley GD. Air and gas drilling manual (3rd Edition). Amsterdam: Elsevier; 2009. p. 293–308.

Marshall DW, Bentsen RG. A computer model to determine the temperature distributions in a wellbore. *J Can Technol*. 1982. doi:10.2118/82-01-05.

Sheffield JS, Sitzman JJ. Air drilling practices in the midcontinent and rocky mountain areas. In: SPE/IADC drilling conference, 5–8 Mar, New Orleans, Louisiana, 1985. doi:10.2118/13490-MS.

Wang C, Meng Y, Jiang W, Deng H. Variation in wellbore temperature and its effects on gas injection rate. *Nat Gas Ind*. 2007;27(10):67–9 (in Chinese).

Wang Y, Meng Y, Li G, Li Y, Liu H, Zhang W, Chen Y. Research on the influence of gas drilling on penetration rate. *J Drill Prod Technol*. 2008;31(2):20–3 (in Chinese).

Wooley GR. Computing downhole temperatures in circulation, injection, and production wells. *JPT*. 1980. doi:10.2118/8441-PA.

Zhang H, Gao D, Salehi S, Guo B. Effect of fluid temperature on rock failure in borehole drilling. *ASCE J Eng Mech*. 2014;140(1):82–90. doi:10.1061/(ASCE)EM.1943-7889.0000648.

Zhang H, Zhang H, Guo B, Gang M. Analytical and numerical modeling reveals the mechanism of rock failure in gas UBD. *J Nat Gas Sci Eng*. 2012;4:29–34. doi:10.1016/j.jngse.2011.09.002.

Zhang Y, Pan L, Pruess K, Finsterle S. A time-convolution approach for modeling heat exchange between a wellbore and surrounding formation. *Geothermics*. 2011;40:261–6. doi:10.1016/j.geothermics.2011.08.003.